

Effect of Vertical Dipole Temperature Anomalies on Convection in a Cloud Model

MARJA BISTER*

Finnish Meteorological Institute, and Division of Atmospheric Sciences, Department of Physical Sciences, University of Helsinki, Helsinki, Finland

BRIAN E. MAPES

NOAA-CIRES Climate Diagnostics Center, Boulder, Colorado

(Manuscript received 14 November 2002, in final form 5 January 2004)

ABSTRACT

A cloud-resolving model is used to study the effects of a vertical temperature dipole on convective cloud development. Such dipole anomalies, with a warm-above-cool structure in the troposphere, are known to be forced by mesoscale convective systems (MCSs) in the Tropics. The experiments involve letting convection develop in perturbed initial soundings with open lateral boundary conditions. Convection is driven solely by surface fluxes. In the control run, a field of deep convection ensues. With a strong dipole anomaly that is warm in the upper troposphere, no clouds ascend beyond the middle troposphere. In this case, cumulus congestus clouds strongly moisten the midtroposphere with relative humidity increases by up to 24% by the end of the 6-h simulation. With a half-strength anomaly, a mixed population results: mainly middle-topped congestus clouds, but with some intermittent deep cells. The partitioning between cloud types is somewhat sensitive to model resolution, with a change from 1- to 0.5-km grid spacing resulting in relatively more congestus clouds and fewer deep cells.

1. Introduction

Convective cloud development is known to depend strongly on the profile of ambient thermodynamic conditions, otherwise known as the sounding. In simulations with cloud models, a tropical mean sounding is often used, but the variability (and uncertainty) about that mean may be too important to ignore. Fluctuations in the temperature profile occur in the vicinity of time-varying heat sources, and since many convective clouds grow in disturbed areas, the formation and structure of many clouds may be affected by neighboring convective systems. In particular, the top heaviness of the heating profile in mesoscale convective systems (MCSs) implies a dynamical forcing for the second vertical mode of the troposphere, with vertical wavelength near the troposphere depth. This top heaviness reflects the heating-over-cooling profile typical of the stratiform regions of MCSs (Houze 1989, 1997), and dynamically induces

dipole fluctuations of temperature with a node in the middle troposphere.

Such dynamically induced temperature changes by MCSs are illustrated by the results of Mapes and Houze (1995), who applied an observationally based top-heavy heating characteristic of MCSs as impulsive thermal forcing in a linearized primitive equation model. The results showed a wavefront of deep subsidence warming propagating at about 50 m s^{-1} , and a warm-over-cold second-mode structure, propagating at about 24 m s^{-1} . Owing to its slower propagation, the second-mode wavefront tends to have especially prominent effects in the near field of such an MCS-like heat source. These effects include vertical-dipole displacements of both potential temperature and humidity isopleths. Cooling and moistening of the lower troposphere by upward displacement could enhance subsequent convection, as suggested by Mapes (1993). However, the associated upper-level subsidence warming and drying will have some effect as well. A model is needed to predict the actual response of convection to such vertical-dipole anomalies.

A larger context for these issues of soundings, convection, and cloud modeling strategy is as follows. On a global (or global Tropics) basis, the forcing for convection is radiative cooling with a fairly constant profile with height. The upper-tropospheric cooling is balanced

* Current affiliation: Division of Atmospheric Sciences, Department of Physical Sciences, University of Helsinki, Helsinki, Finland.

Corresponding author address: M. Bister, Dept. of Physical Sciences, University of Helsinki, Physicum C406, P.O. Box 64, FIN-00014 Helsinki, Finland.
E-mail: marja.bister@helsinki.fi

by top-heavy heating in MCSs (see Fig. 1 of Mapes 2000), while the lower-tropospheric cooling is balanced by lower-tropospheric heating by shallow to middle-depth convection, which is typically not organized into mesoscale cloud masses like MCSs. In order to simulate MCSs in a limited-domain cloud model, it may be necessary to impose a top-heavy destabilization profile (cooling), or in the case of an initial-sounding approach, a top-heavy initial instability profile, in order to provoke development of convective process with a top-heavy heating. By a similar token, to simulate unorganized convection only, one might want to cool the lower troposphere preferentially in the model's initial sounding or forcing profile. Which comes first, lower-tropospheric convection or MCSs with stratiform precipitation and top-heavy heating, is unclear. However, their complementarity is clear, and both excite dynamical variability involving the second vertical mode of the troposphere, which would otherwise not be prominent (section 3e of Mapes 2001).

Within this complementary nonlocal partnership between stratiform precipitation in MCSs and middle-topped cumulus clouds, the former is by far the more extensively studied member. As a small remedy to this imbalance, this paper describes the use of a cloud-resolving model to study cumulus congestus clouds, enhanced by second-vertical-mode temperature anomalies in the initial sounding.

Convective cloud modeling raises a number of subtle issues involving boundary and initial conditions, discussed more thoroughly in section 2, but some discussion is pertinent here. Two common tactics for convective cloud modeling are initial-condition experiments, in which a preconvective sounding is specified; and equilibrium experiments, in which the sounding develops out of the balance between convection and its forcing. Equilibrium experiments tend to use periodic boundary conditions, which are very clean and well posed, while initial-condition experiments are often done with so-called open lateral boundary conditions. Open boundaries are imperfect, but tend to reduce a major problem with periodic domains: that convection excessively alters its own environment, through trapping of the heating-induced subsidence wavefronts within the domain. With initial-condition experiments one can also choose to force the convection with surface fluxes, thus avoiding imposing vertical structures associated with other kinds of forcing typically used in equilibrium experiments.

In this work, an initial-condition, open-boundary approach is used to study the effect of second-mode temperature anomalies on convection. The experiments are simple: we perturb the observationally based initial sounding and allow convection to develop during a short (6 h) integration. One possible shortcoming of this approach is that the sensitivities of the model cloud field are assessed in a slightly unnatural setting: clouds developing into a too-homogeneous environment with a

sounding that is foreign to the model's natural "climate." However, the experiments span an interesting range and our main results are comparative, so this shortcoming is not fatal. Complementary experiments using an equilibrium approach and periodic boundary conditions are described in Mapes (2004, hereafter M04).

In section 2, the model and the design of the experiments are described. In section 3, results are discussed. In section 4, formation of congestus clouds is discussed in a larger context and conclusions are drawn in section 5.

2. Model and experiment setup

Our simulations use the Advanced Regional Prediction System (ARPS) model (Xue et al. 2000, 2001), which has nonhydrostatic compressible dynamics and a choice of physics options. The $120 \text{ km} \times 120 \text{ km}$ three-dimensional domain has a horizontal grid spacing of 1000 m, with a few sensitivity tests run at 500-m grid spacing. The vertical grid spacing is fixed to 334 m. A mode splitting technique is used for the time integration, with a large time step (8 s) for leapfrog time integration of the nonacoustic wave modes and a 1-s time step for acoustic waves. Advection is fourth order in the horizontal and second order in the vertical direction. Mixing parameterizations include a 1.5-level turbulence kinetic energy formulation (Xue et al. 2000), as well as fourth-order computational smoothing.

The upper and lower boundary conditions are rigid surfaces. Rayleigh damping is used in a sponge layer extending from 15 km to the model top at 19.2 km. Coriolis terms are set to zero. The ice microphysics is from Tao and Simpson (1993), with Kessler warm rain microphysics and three-category ice-phase (cloud ice, snow, and hail/graupel) parameterization schemes from Lin et al. (1983). No radiation is applied in the model simulations. Surface fluxes are calculated using constant surface drag coefficients and specified values of sea surface potential temperature (302.5 K) and relative humidity (100%). The temperature field is initially horizontally homogeneous and no wind is initially present.

We have chosen to use open boundary conditions so that convectively induced gravity waves (and the associated "compensating subsidence") can leave the mesoscale domain of the model simulations. With the other common choice, periodic boundary conditions, the trapping of compensating motions would cause the model sounding to be heated and stabilized too quickly by the latent heating associated with the *local* cloud field. The use of open boundary conditions tends to maintain the model's sounding close to the initial, realistic sounding even as convection is allowed to operate for several hours.

To minimize problems associated with convection occurring too close to lateral boundaries of the model domain, surface fluxes of moisture are not allowed in the outer domain within 35 km from the boundaries. This

quite efficiently prevents convection within the outer domain. The full integration domain is 120 km in both horizontal directions, so convection occurs roughly in a domain of $50 \text{ km} \times 50 \text{ km}$.

The goal of studying the effect of height-dependent temperature anomalies also sets requirements for the forcing for convection. Using a height-dependent forcing (representing radiative cooling or vertical motion) would affect the vertical structure of convection, so separating the effects of the initial temperature anomalies and the vertical structure of the forcing would be difficult. Therefore, we have chosen to apply the forcing from the surface by applying a minimum wind speed of 14 m s^{-1} in the sea surface flux formulations. The minimum wind speed results in sea surface fluxes of latent and sensible heat of 290 and 45 W m^{-2} initially, respectively. Thus, the only imposed vertical structures are those associated with the initial (realistic) sounding, plus the second-mode temperature anomalies, which vary from experiment to experiment.

At the two lowest model levels (at the altitudes of 167 and 501 m) a random field of temperature forcing is applied within the inner integration domain following Tao and Soong (1986). Values of 0.5 K or less in magnitude are added to the temperature field over the time period of 6 min. Every 6 min, a new random forcing field is generated. The horizontal average of the forcing is zero at all times. Using this method results in a smoother integration with convection initiating earlier.

The model is initialized using the mean sounding from Tropical Ocean Global Atmosphere Coupled Ocean–Atmosphere Response Experiment (TOGA COARE; Zuidema 1998) with the water vapor mixing ratio increased by 5% in the lowest 100 hPa to crudely account for the measurement error of the relative humidity in the boundary layer (e.g., Guichard et al. 2000; Wang et al. 2002).

With the specified initial sounding, these simulations can be characterized as spindown (or spinup) as opposed to equilibrium experiments (Emanuel 1994). Because the initial sounding is a mean of many soundings, it is not a true preconvective sounding. Furthermore, even for a given sounding, the effective moist convective instability in the model is not necessarily the same as it is in nature. The reason for this difference is that the buoyancy of model updrafts, which controls the development of convection, depends on imperfectly parameterized mixing and microphysical processes. Another choice would be to run the model into a radiative–convective equilibrium in which process the model would create a model-consistent initial sounding. However, the resulting sounding would probably depend strongly on the morphology of convection, which could deviate from that in nature. In current simulations, the model convection only develops gradually while the strong surface fluxes destabilize the atmosphere. The spinup problem undoubtedly affects the quantitative results from this study, but not their qualitative sense.

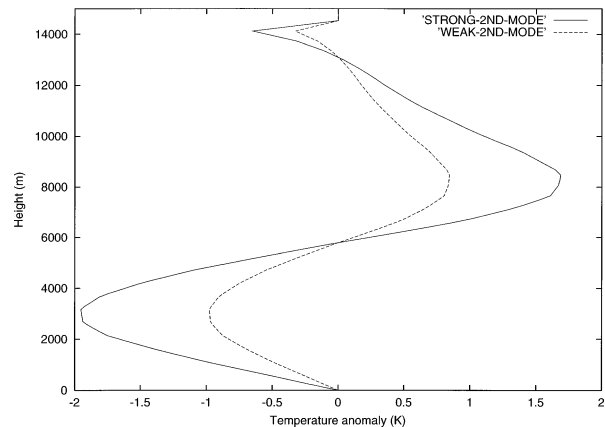


FIG. 1. Second-vertical-mode temperature anomalies used in the model experiments.

In the experiments, we use second-mode temperature anomalies from the Fulton and Schubert (1985) vertical transform applied to the mean TOGA COARE sounding, as discussed by Mapes (1998). It is important to note that these anomalies are characteristic of a dynamical mode of the atmosphere (within certain assumptions—hydrostatic, upper boundary, etc.) Because atmospheric waves are strongly dispersive with respect to vertical wavelength, even heating fluctuations whose profiles are not modal in structure, like cumulus congestus heating confined to the lower troposphere, will tend to generate temperature fluctuations with modal vertical structure. For more discussion, see Mapes and Houze (1995) and Mapes (1998). The strong second-mode temperature anomaly reaches a maximum of 1.7 K at the height of 8.4 km and a minimum of -1.95 K at the height of 3.2 km (Fig. 1), magnitudes that are about twice the standard deviation of temperature in the tropical free troposphere. The weaker second-mode temperature anomalies used in the experiments are half as great (Fig. 1).

These second-mode temperature anomalies are applied from the start of the simulation and are in principle free to vanish in time, but they do not (as will be discussed in section 3). Because these temperature anomalies reflect vertical displacements by wave motions, they should perhaps, for consistency, be associated with corresponding anomalies in moisture. For simplicity, initial moisture changes are omitted from the model. Since the moisture field evolves so much, both in the mean and in the development of fine structure (e.g., clouds), the effects of modest initial moisture perturbations would be difficult to interpret. In the experiments of M04, the effects of moisture and temperature anomalies associated with vertical displacements on rainfall rate are found to be about equal in the case of a first-vertical-mode vertical displacement.

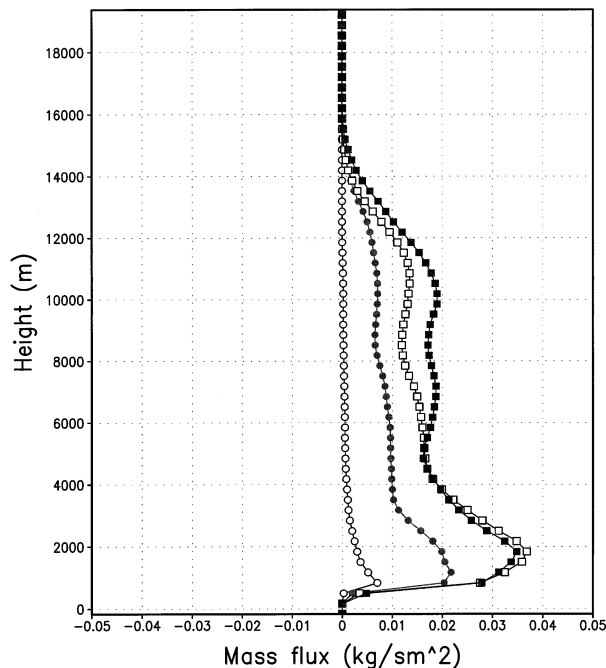


FIG. 2. Averaged cloud upward mass fluxes within the inner domain in the experiment without second-mode temperature anomalies. Mass flux averages are calculated using 12-min model output between 0 and 3 h (open circle), 3 and 6 h (filled circle), 6 and 9 h (open square), and 9 and 12 h (filled square).

3. Results

a. Sensitivity of convection to second-mode temperature anomalies

Figure 2 shows the area-averaged cloud upward mass flux within the inner domain (i.e., excluding the 35-km-wide boundary zone) in the control simulation. The mean mass flux in cloudy grid points with positive vertical velocity was calculated and the result was multiplied by the ratio of the number of such grid points to the total number of grid points. The time averages were calculated using instantaneous mass flux values obtained every 12 min.

It takes several hours for convection to spin up in the model. Between 0 and 3 h, the mean cloud mass flux is still small. Between 3 and 6 h, the mass flux is already about half of that between 6 and 9 h or 9 and 12 h. We have chosen to study the fields between 3 and 6 h more closely. This choice for the time interval is a compromise between the goal of studying the initial effect of the temperature anomalies on convection, before feedbacks become too complicated, and on the other hand, of minimizing spinup problems.

It is interesting to compare the magnitude of the mass fluxes in Fig. 2 to those obtained in cloud-resolving simulations of convection in radiative-convective equilibrium. In experiments made by Robe and Emanuel (1996), the upward cloud mass flux is about $0.015 \text{ kg s}^{-1} \text{ m}^{-2}$ for a radiative cooling rate of 2.1 K day^{-1} .

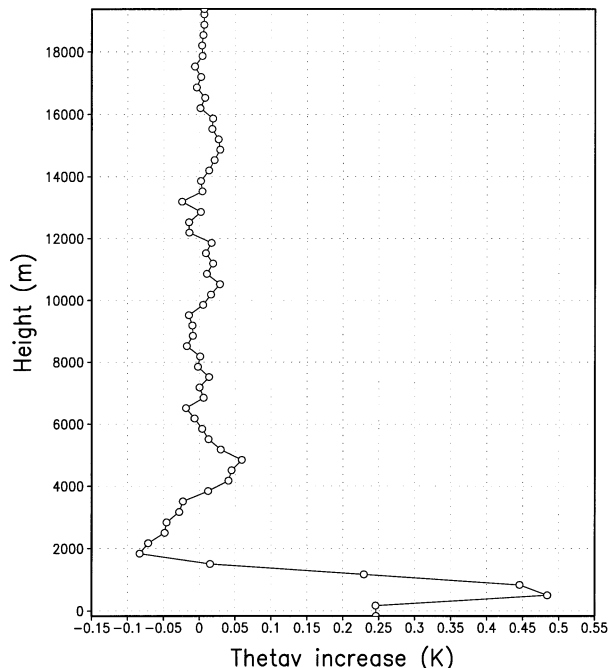


FIG. 3. Increase of the mean virtual potential temperature in 6 h within the inner domain in the experiment with no second-mode temperature anomalies.

The mass flux between 3 and 6 h (Fig. 2) is somewhat smaller at most altitudes but of the same order of magnitude. Thus, the large value used for the minimum wind speed in the calculation of surface fluxes does not result in an excessive upward mass flux in clouds.

The mean virtual potential temperature increase during the first 6 h of the control simulation is shown in Fig. 3. Apart from the lowest 1.5 km, the change is very small, mostly less than 0.05 K in magnitude. With weak and strong second-mode anomalies, the corresponding change is less than 0.05 and 0.1 K in magnitude, respectively (not shown). It can be concluded that the initial temperature structure of the TOGA COARE mean sounding, with or without the imposed temperature anomalies, is well conserved in the model during course of the 6 h.

In case of strong second-mode anomalies, the spinup of convection happens faster (Fig. 4), owing to the 0.7 K km^{-1} destabilization of the lapse rate in the lower troposphere (Fig. 1). The average cloud upward mass flux is almost as large between 0 and 3 h as it is between 3 and 6 h. In contrast, with half-strength anomalies, convection is still spinning up after the first 3 h (Fig. 5). Vertical structures of the cloud mass fluxes in each experiment depend relatively little on time, apart from the first 3 h in the control run, and some modest changes in the upper part of the layers with clouds (6–12 km in Fig. 2; 4–6 km in Fig. 4). Therefore, a qualitative comparison of the vertical structures of the mass fluxes in different experiments is not very sensitive to the time period chosen.

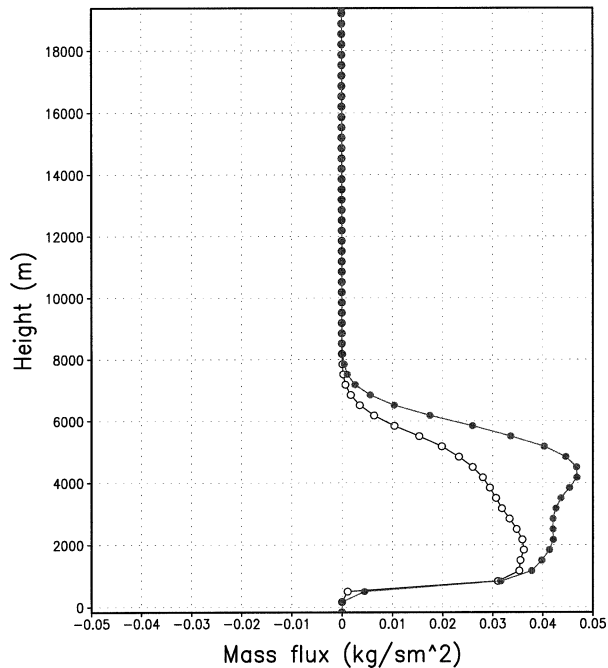


FIG. 4. Same as Fig. 2, but in the experiment with strong second-mode temperature anomalies. Open circles show the average between 0 and 3 h and filled circles between 3 and 6 h.

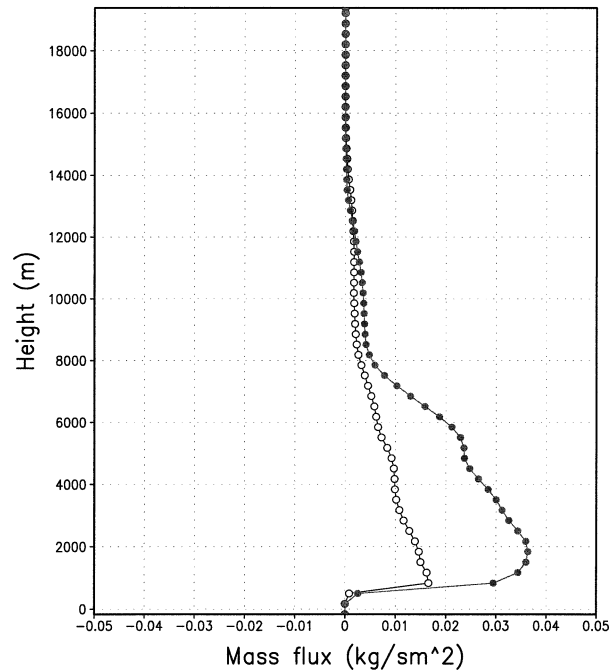


FIG. 5. Same as Fig. 4, but in the experiment with weak second-mode temperature anomalies.

In the control run, the mass flux decreases quite smoothly with height with a small exception being the slight increase in the 8–10-km layer between 6 and 12 h in Fig. 2. The most rapid decreases occur between 2 and 4 km and between 11 and 14 km (Fig. 2), with a weaker but distinct decrease in the 6–8-km layer between 3 and 9 h. In the intermediate case with weak second-mode anomalies (Fig. 5), the decrease of mass flux with height is fairly smooth, but again is enhanced in the 2–4- and 6–8-km layers. Above 8 km, the mass flux is very small and decreases to zero at the altitude of 14 km, but again with the steepest decrease in the 11–14-km layer. With strong anomalies (Fig. 4), the mass flux is large in the lower troposphere and decreases very rapidly above 5 km, with practically no mass flux above the altitude of 8 km.

Inspection of model fields confirms that, in the experiment with strong temperature anomalies, the clouds are predominantly of cumulus congestus type, reaching altitudes less than 8 km (not shown). At the other extreme, the control run contains mostly deep convective clouds that reach well above the altitude of 10 km. In the experiment with weak anomalies, the decrease of mass flux seen in the middle troposphere between 6 and 8 km is mostly associated with congestus clouds with tops in the middle troposphere. Few of the convective clouds penetrate above 10 km. These two cloud types, congestus and deep convective clouds, seem to be responsible for the mass flux profile. Detrainment in the middle troposphere from deep clouds, resulting in

shelves of increased cloudiness at that level, are not evident in the model.

b. Sensitivity of humidity changes to second-mode temperature anomalies

We also examined changes to domain-averaged humidity in the experiments. To crudely reduce the effect of spinup-rate differences on the comparison, the humidity changes at 6 h from the experiments with strong and weak second-mode anomalies are compared to those from the control run at 9 h.

The increase of relative humidity in the three experiments is shown in Fig. 6. In the control run, the predominance of deep convective clouds causes the greatest relative humidity increase (15%) to be in the upper troposphere at 12 km. In the middle troposphere, the increase of relative humidity is modest, about 7% or less, and is nearly zero at 4 km [reminiscent of the results of Zuidema (1998)]. A spike below 2 km is evident in all runs, and is probably due to boundary layer development owing to the large latent heat flux from the surface.

With weak second-mode anomalies, the relative humidity increase in 6 h of simulation time reaches a maximum of 12% at the altitude of 6.5 km. There is a weak local maximum at the altitude of 12 km.

The largest absolute increase occurs in the experiment with strong anomalies. At the altitude of about 6 km, relative humidity has increased in 6 h by 24%, to 85%. The strong moistening in this case is due to two effects.

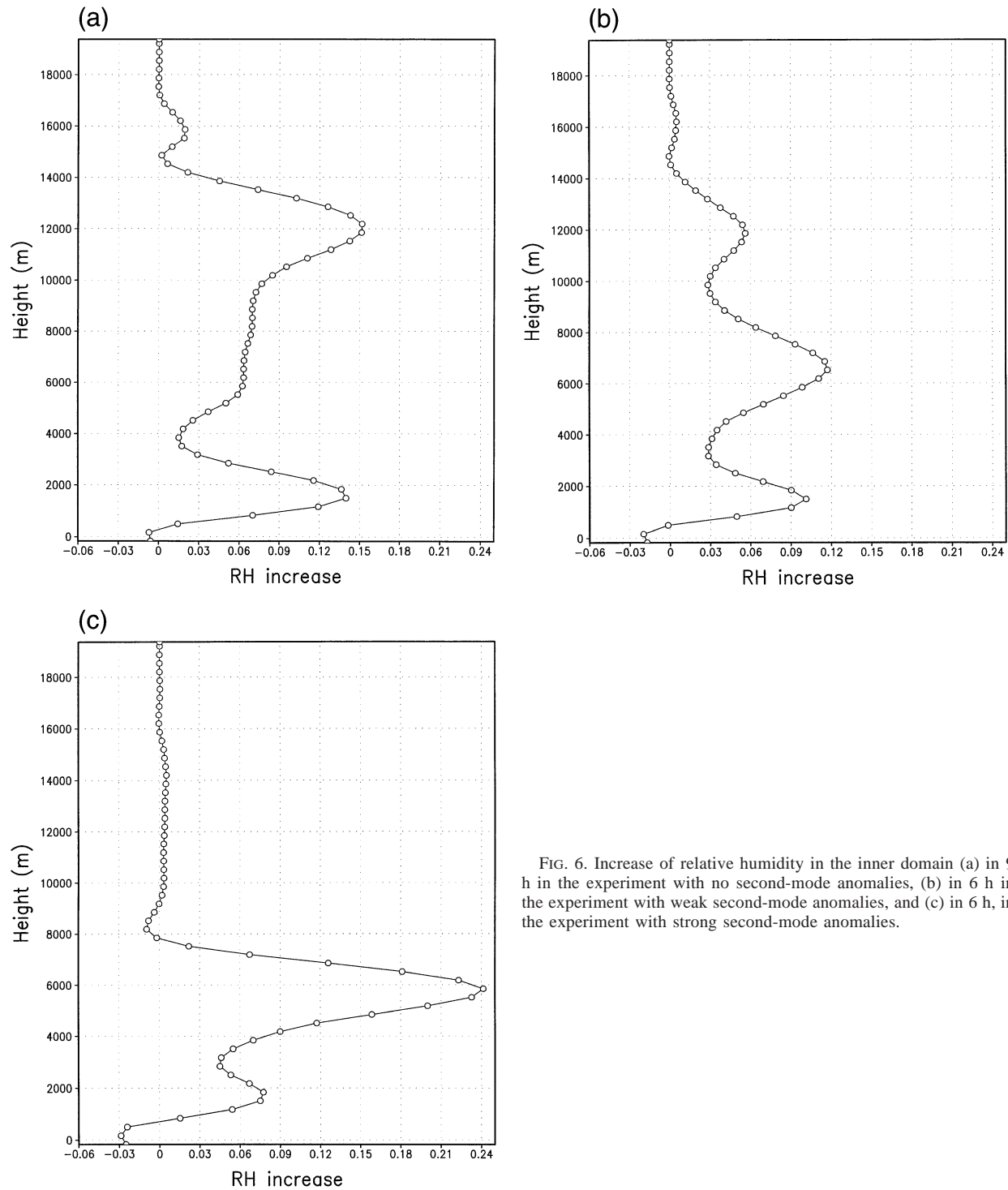


FIG. 6. Increase of relative humidity in the inner domain (a) in 9 h in the experiment with no second-mode anomalies, (b) in 6 h in the experiment with weak second-mode anomalies, and (c) in 6 h, in the experiment with strong second-mode anomalies.

One is the confinement of detrainment in a thin layer of about 2 km in depth. The other is the increased mass flux in the lower troposphere as compared to the control experiment (Figs. 2 and 4). The increased mass flux is a response to the cold part of the second-mode temperature anomaly in the lower troposphere, which enhances convection.

c. Horizontal resolution

The effect of horizontal resolution was studied by using a halved horizontal grid length, 0.5 km, in simulations with no and weak second-mode temperature anomalies. The improved resolution resulted in more congestus and fewer, shorter deep clouds. Perhaps the

higher resolution begins to permit eddies that are important agents of entrainment on cloud scales. Bryan and Fritsch (2001) have suggested that a grid spacing of about 100 m would be needed in cloud modeling studies so that the simulated flow could become fully turbulent. Carpenter et al. (1998) used 50 m for their study of individual "cumulus congestus" clouds, although in their case this meant clouds of less than 3 km in depth, with no ice or precipitation processes. Unfortunately, our computer resources did not allow using such a fine-grid spacing.

4. Discussion of formation of congestus clouds

Cumulus congestus clouds were estimated to contribute to 28% of the total convective rainfall and 57% of the precipitating convective clouds in TOGA COARE (Johnson et al. 1999). In that study, congestus clouds were defined to be those convective clouds with tops between 4.5 and 9.5 km, similar to the clouds examined here, but considerably deeper than the nonprecipitating clouds of the same name examined by Carpenter et al. (1998). Those authors also reviewed earlier work showing that midtropospheric detrainment and radar-echo tops are common in other tropical regions. Also, recent observations of the vertical structure of rain over the whole Tropics using a precipitation radar aboard the Tropical Rainfall Measuring Mission (TRMM) satellite show a strongly bimodal distribution, with a prominent contribution by low-to-middle depth clouds (Short and Nakamura 2000).

Johnson et al. (1999) showed that congestus clouds in TOGA COARE were *most prevalent* when there was MCS organization and cumulonimbus activity. The existence of mixed populations raises the question of what prevents some clouds from reaching the upper troposphere, or (the other way around) what allows some clouds to reach the upper troposphere when many do not?

One suggestion for the prevalence of middle-topped convective clouds is to invoke the observed stable (roughly isothermal) layer near the 0°C temperature level, associated with precipitation melting (Johnson et al. 1996). However, the thinness of this layer of enhanced stability, and the existence of an associated anomalously low stability just below it, as well as the mismatch of some kilometers between the height of the 0°C level and the top heights of congestus clouds, raise doubts about this simple interpretation. Another suggestion comes from the work of Zuidema (1998) utilizing the buoyancy sorting model of Raymond and Blyth (1992). She found that, if no ice processes were allowed, many parcels reached neutral buoyancy close to 400 hPa. In the opposite extreme, with ice processes occurring at thermodynamic equilibrium, very few did. Since nature lies in between these, subtle issues of the internal structure of convective clouds may be involved.

Our experiments show that warm-over-cold temper-

ature anomalies, of the sort that may develop in response to MCS-like heat sources, enhance the formation of congestus clouds, consistent with simple ideas of updraft buoyancy. This effort follows the suggestion of Johnson et al. (1996) that *some* of the observed stable layers near the 0°C level could be associated with second-vertical-mode temperature anomalies forced by a top-heavy heating structure in MCSs (e.g., Houze 1989, 1997). For example, the case study of Johnson et al. (1995) highlights evidence of flow structures between two MCSs that resembled those associated with gravity waves emanating from MCS-like convective heat sources. The gravity wave-induced subsidence aloft and ascent in the lower troposphere in that case enhanced an inversion in the middle troposphere and resulted in development of vigorous congestus clouds between the MCSs, as in our model results. Although this was a dramatic case, it is possible that the prevalence of congestus clouds in MCS conditions more generally is at least partly due to second-vertical-mode temperature anomalies forced by MCS heating.

5. Summary and conclusions

We used the cloud-resolving ARPS model to study how the vertical dipole temperature anomalies (Fig. 1) can affect the vertical structure of convection. More specifically, we cooled the lower troposphere and warmed the upper troposphere in the initial sounding. Our rationale for these experiments (discussed in the introduction) is that such anomalies are forced by tropical MCSs, and propagate as waves which act to intermingle the top-heavy heating in MCSs and the bottom-heavy heating in precipitating cumulus congestus clouds into a deep profile that balances radiative cooling in tropical radiative-convective equilibrium. To focus our investigation on unorganized, shallower convection rather than MCSs with stratiform precipitation, we chose to apply second-vertical-mode temperature anomalies of the sign used here.

In our control run, a field of deep convection ensues. With strong second-mode anomalies, no deep clouds form but congestus clouds are abundant. With weak second-mode anomalies, the ensuing cloud field is mixed, comprised mostly of congestus clouds, but some clouds are able to reach altitudes well above 10 km.

The effect of second-mode anomalies on relative humidity was strong and clear, although its quantitative magnitude does depend on the spinup process in these initial-condition experiments. The experiment with stronger second-mode temperature anomalies, having vigorous congestus clouds, exhibited a strong midtropospheric moistening. With no second-mode anomalies, the largest increase of relative humidity occurred around the altitude of 12 km, with modest moistening in the midtroposphere. With the maximum temperature anomaly roughly equaling the standard deviation of temperature in the Tropics (weak second mode), the 6-h relative

humidity increase reaches a maximum of 12% at the altitude of 6.5 km. With the maximum temperature anomaly about twice the standard deviation of temperature in the Tropics (strong second mode), relative humidity increases by 24% at the altitude of about 6 km in 6 h of simulation time. This moistening is remarkable, given the relatively modest cloud upward mass flux (corresponding to less than 10 K day⁻¹ of heating). The strong moistening in that case is due to two effects, the confinement of detrainment in a thin layer (about 2 km in depth) and the increased mass flux in the lower troposphere as compared to the control experiment. The increased mass flux, in turn, is a response to the cold part of the second-mode temperature anomaly in the lower troposphere, which enhances convection.

Recent model studies have pointed to the important role of low- to midtropospheric moisture in enhancing and organizing convection (e.g., Raymond 2000; Lucas et al. 2000; Tompkins 2001; Grabowski 2003). Moistening of the low to midtroposphere is likely to affect future convection through weakening of evaporative downdrafts and moister air being entrained into the clouds (e.g., Raymond 1995; Tompkins 2001). Moreover, observational studies show a clear link between moisture and deep convection (e.g., Brown and Zhang 1997; Sherwood 1999; Kingsmill and Houze 1999). In the light of these studies, the rapid increase of the midtropospheric moisture observed in the experiment with strong second-mode temperature anomalies can have important consequences for subsequent convection. Moreover, an interesting question is whether there could be a positive feedback with a top-heavy heating profile associated with MCSs enhancing the occurrence of congestus clouds, which, detrains moisture in the middle-tropospheric base level of MCS stratiform anvils.

As we still do not know which is more important for the formation of congestus clouds in the real atmosphere—the second-mode anomalies or the thinner stability anomalies as would be caused by melting of snow at the 0°C level—experiments similar to those reported here should be conducted to study the effect of thinner stability anomalies on fields of convective clouds.

A few experiments with a 0.5-km horizontal grid length cautioned that the quantitative results are sensitive to resolution. Specifically, improving the resolution resulted in lower cloud tops. As Kingsmill and Houze (1999) found that the inflow air to deep convection was significantly moister above 1-km altitude than the inflow air to shallow convection, it would be interesting to study whether increased moisture in the lower troposphere would aid in the formation of deeper clouds in experiments with finer resolution.

Acknowledgments. The simulations were made using the Advanced Regional Prediction System (ARPS) developed by the Center for Analysis and Prediction of Storms (CAPS), University of Oklahoma. CAPS is supported by the National Science Foundation and the Fed-

eral Aviation Administration under Grant ATM92-20009. Many of the figures were produced with GrADS, originally developed by Brian Doty of Center for Ocean–Land–Atmosphere Studies (COLA). The authors would like to thank Wojtek Grabowski and an anonymous reviewer for their comments and questions that significantly improved the manuscript. Marja Bister was supported by the Academy of Finland. Brian Mapes was supported by NSF grant.

REFERENCES

- Brown, R. G., and C. Zhang, 1997: Variability of midtropospheric moisture and its effect on cloud-top height distribution during TOGA COARE. *J. Atmos. Sci.*, **54**, 2760–2774.
- Bryan, G. H., and J. M. Fritsch, 2001: On adequate resolution for the simulation of deep moist convection: Theory and preliminary simulations. Preprints, *Ninth Conf. on Mesoscale Processes*, Fort Lauderdale, FL, Amer. Meteor. Soc., 288–292.
- Carpenter, R. L., Jr., K. K. Droegemeier, and A. M. Blyth, 1998: Entrainment and detrainment in numerically simulated cumulus congestus clouds. Part I: General results. *J. Atmos. Sci.*, **55**, 3417–3432.
- Emanuel, K. A., 1994: *Atmospheric Convection*. Oxford University Press, 580 pp.
- Fulton, S. R., and W. H. Schubert, 1985: Vertical normal mode transforms: Theory and application. *Mon. Wea. Rev.*, **113**, 647–658.
- Grabowski, W. W., 2003: MJO-like coherent structures: Sensitivity simulations using the Cloud-Resolving Convection Parameterization (CRCP). *J. Atmos. Sci.*, **60**, 847–864.
- Guichard, F., D. Parsons, and E. Miller, 2000: Thermodynamic and radiative impact of the correction of sounding humidity bias in the Tropics. *J. Climate*, **13**, 3611–3624.
- Houze, R. A., 1989: Observed structure of mesoscale convective systems and implications for large-scale heating. *Quart. J. Roy. Meteor. Soc.*, **115**, 425–461.
- , 1997: Stratiform precipitation in regions of convection: A meteorological paradox? *Bull. Amer. Meteor. Soc.*, **78**, 2179–2196.
- Johnson, R. H., B. D. Miner, and P. E. Ciesielski, 1995: Circulations between mesoscale convective systems along a cold front. *Mon. Wea. Rev.*, **123**, 585–599.
- , P. E. Ciesielski, and K. A. Hart, 1996: Tropical inversions near the 0°C level. *J. Atmos. Sci.*, **53**, 1838–1855.
- , T. M. Rickenbach, S. A. Rutledge, P. E. Ciesielski, and W. H. Schubert, 1999: Trimodal characteristics of tropical convection. *J. Climate*, **12**, 2397–2418.
- Kingsmill, D. E., and R. A. Houze Jr., 1999: Thermodynamic characteristics of air flowing into and out of precipitating convection over the west Pacific warm pool. *Quart. J. Roy. Meteor. Soc.*, **125**, 1209–1229.
- Lin, Y. L., R. D. Farley, and H. D. Orville, 1983: Bulk parameterization of the snow field in a cloud model. *J. Climate Appl. Meteor.*, **22**, 1065–1092.
- Lucas, C., E. J. Zipser, and B. S. Ferrier, 2000: Sensitivity of tropical West Pacific oceanic squall lines to tropospheric wind and moisture profiles. *J. Atmos. Sci.*, **57**, 2351–2373.
- Mapes, B. E., 1993: Gregarious tropical convection. *J. Atmos. Sci.*, **50**, 2026–2037.
- , 1998: The large-scale part of tropical mesoscale convective system circulations: A linear vertical spectral band model. *J. Meteor. Soc. Japan*, **76**, 29–55.
- , 2000: Convective inhibition, subgrid-scale triggering, and stratiform instability in a simple tropical wave model. *J. Atmos. Sci.*, **57**, 1515–1535.
- , 2001: Water's two height scales: The moist adiabat and the radiative troposphere. *Quart. J. Roy. Meteor. Soc.*, **127**, 2253–2266.
- , 2004: Sensitivities of cumulus-ensemble rainfall in a cloud-

- resolving model with parameterized large-scale dynamics. *J. Atmos. Sci.*, in press.
- , and R. A. Houze Jr., 1995: Diabatic divergence profiles in Western Pacific mesoscale convective systems. *J. Atmos. Sci.*, **52**, 1807–1828.
- Raymond, D. J., 1995: Regulation of moist convection over the west Pacific warm pool. *J. Atmos. Sci.*, **52**, 3945–3959.
- , 2000: Thermodynamic control of tropical rainfall. *Quart. J. Roy. Meteor. Soc.*, **126**, 889–898.
- , and A. M. Blyth, 1992: Extension of the stochastic mixing model to cumulonimbus clouds. *J. Atmos. Sci.*, **49**, 1968–1983.
- Robe, F. R., and K. A. Emanuel, 1996: Moist convective scaling: Some inferences from three-dimensional cloud ensemble simulations. *J. Atmos. Sci.*, **53**, 3265–3275.
- Sherwood, S. C., 1999: Convective precursors and predictability in the tropical Western Pacific. *Mon. Wea. Rev.*, **127**, 2977–2991.
- Short, D. A., and K. Nakamura, 2000: TRMM radar observations of shallow precipitation over the tropical oceans. *J. Climate*, **13**, 4107–4124.
- Tao, W. K., and S.-T. Soong, 1986: A study of the response of deep tropical clouds to mesoscale processes: Three-dimensional numerical experiments. *J. Atmos. Sci.*, **43**, 2653–2676.
- , and J. Simpson, 1993: Goddard cumulus ensemble model. Part I: Model description. *Terr. Atmos. Oceanic Sci.*, **4**, 35–72.
- Tompkins, A. M., 2001: Organization of tropical convection in low vertical wind shears: The role of water vapor. *J. Atmos. Sci.*, **58**, 529–545.
- Wang, J., H. L. Cole, D. J. Carlson, E. R. Miller, K. Beierle, A. Paukkunen, and T. K. Laine, 2002: Corrections of humidity measurement errors from the Vaisala RS80 radiosonde—Application to TOGA COARE data. *J. Atmos. Oceanic Technol.*, **19**, 981–1002.
- Xue, M., K. K. Droegemeier, and V. Wong, 2000: The Advanced Regional Prediction System (ARPS): A multi-scale nonhydrostatic atmospheric simulation and prediction model. Part I: Model dynamics and verification. *Meteor. Atmos. Phys.*, **75**, 161–193.
- , and Coauthors, 2001: The Advanced Regional Prediction System (ARPS)—A multi-scale nonhydrostatic atmospheric simulation and prediction tool. Part II: Model physics and applications. *Meteor. Atmos. Phys.*, **76**, 143–165.
- Zuidema, P., 1998: The 600–800-mb minimum in tropical cloudiness observed during TOGA COARE. *J. Atmos. Sci.*, **55**, 2220–2228.